Brain Pathology ISSN 1015-6305

RESEARCH ARTICLE

Degree of Cajal–Retzius Cell Mislocalization Correlates with the Severity of Structural Brain Defects in Mouse Models of Dystroglycanopathy

Helen S. Booler; Josie L. Williams; Mark Hopkinson; Susan C. Brown

Department of Comparative Biomedical Sciences, Royal Veterinary College, London, UK.

Keywords
Cajal–Retzius cells, congenital muscular dystrophy, dystroglycan, neuronal migration, pial basement membrane, reelin.

Corresponding author:
Susan C. Brown, BSc(hons), PhD, Department of Comparative Biomedical Sciences, Royal Veterinary College, London NW1 0TU, UK (E-mail: *scbrown@rvc.ac.uk*)

Received 30 March 2015
Accepted 23 August 2015
Published Online Article Accepted 26 August 2015

doi:10.1111/bpa.12306

Abstract

The secondary dystroglycanopathies are characterized by the hypoglycosylation of alpha dystroglycan, and are associated with mutations in at least 18 genes that act on the glycosylation of this cell surface receptor rather than the *Dag1* gene itself. At the severe end of the disease spectrum, there are substantial structural brain defects, the most striking of which is often cobblestone lissencephaly. The aim of this study was to determine the gene-specific aspects of the dystroglycanopathy brain phenotype through a detailed investigation of the structural brain defects present at birth in three mouse models of dystroglycanopathy—the $FKRP^{KD}$, which has an 80% reduction in *Fkrp* transcript levels; the $Pomgnt1_{null}$, which carries a deletion of exons 7–16 of the *Pomgnt1* gene; and the $Large^{myd}$ mouse, which carries a deletion of exons 5–7 of the *Large* gene. We show a rostrocaudal and mediolateral gradient in the severity of brain lesions in $FKRP^{KD}$, and to a lesser extent $Pomgnt1_{null}$ mice. Furthermore, the mislocalization of Cajal–Retzius cells is correlated with the gradient of these lesions and the severity of the brain phenotype in these models. Overall these observations implicate gene-specific differences in the pathogenesis of brain lesions in this group of disorders.

INTRODUCTION

The dystroglycanopathies are a heterogeneous group of neuromuscular diseases, associated with mutations in genes that encode proteins implicated in the glycosylation of alpha dystroglycan (DG) rather than the *Dag1* gene itself. As a consequence, these are referred to as "secondary" rather than primary. Rare mutations in the *Dag1* gene have been reported, but they amount to only a few cases due most likely to embryonic lethality (26). To date, mutations in at least 18 genes have been associated with the secondary dystroglycanopathies, many of which encode either proven or putative glycosyltransferases. These include POMGNT1, which is a demonstrated glycosyltransferase adding N-acetylglucosamine (86); LARGE, a bifunctional glycosyltransferase that alternately transfers xylose and glucuronic acid and confers ligand binding (24, 37, 49, 78); and Fukutin-related protein (FKRP), the function of which is currently unknown (6, 9, 11). Interestingly, mutations in these genes are associated with a wide spectrum of clinical phenotypes, which at the severe end of the disease spectrum include congenital muscular dystrophies with structural brain defects, exemplified by Walker–Warburg syndrome (WWS) OMIM 236670, muscle eye brain disease (MEB) OMIM 253280, congenital muscular dystrophy type 1C OMIM 606612 and congenital muscular dystrophy type 1D OMIM 608840. Severely affected patients typically show a range of structural brain abnormalities associated with defects in neuronal migration, particularly type II (cobblestone) lissencephaly, which is strongly suggestive of this group of disorders (16). In addition, patients may show cortical and cerebellar dysplasia, polymicrogyria and hydrocephalus, with evidence of dysmyelination on magnetic resonance imaging (8). Work in dystroglycanopathy patients and mouse models strongly suggests that the hypoglycosylation of alpha DG is central to the pathogenesis via its effect on the structural integrity of the pial basement membrane during cortical development (55, 58).

DG is transcribed from a single gene (*Dag1*) and undergoes post-translational cleavage to produce the peripheral membrane protein alpha DG, and the transmembrane protein beta DG, which are non-covalently linked (36). Alpha DG undergoes extensive O-linked mannosylation of its central mucin-rich domain, and these glycan chains mediate binding to extracellular matrix proteins such as laminin (19), agrin (22, 85), neurexin (73), pikachurin (68) and perlecan (56). Beta DG in turn interacts with the cell's actin cytoskeleton via dystrophin, utrophin, ezrin or plectin (56). Together, alpha and beta DG effectively link the cytoskeleton to the extracellular matrix. The DG complex has been previously demonstrated to play a primary role in the deposition, organization and turnover of basement membranes (30).

Targeted deletion of DG in the brain during development, or mutations of known or putative glycosyltransferases involved in the glycosylation of alpha DG, have both been demonstrated previously to recapitulate many aspects of WWS and MEB, indicating DG as central to the disease pathogenesis (1, 24, 48, 57). However, in the absence of comparative studies it is unclear whether some

aspects of the neuropathologic lesions are gene specific. In order to answer this question, we have now undertaken a detailed investigation of the structural brain defects in three dystroglycanopathy mouse models—the FKRP-Neo^{Tyr307Asn} (FKRP^{KD}), which has an 80% reduction in *Fkrp* transcript levels (1); the Pomgnt1$_{null}$ mouse, which carries a deletion of exons 7–16 of the *Pomgnt1* gene; and the Large^{myd} mouse, which carries a deletion of exons 5–7 of the *Large* gene (24).

MATERIALS AND METHODS

Mouse models and genotyping

Three dystroglycanopathy mouse models were compared: the FKRP-Neo^{Tyr307Asn} (FKRP^{KD}) (1), the Pomgnt1$_{null}$ and the Large^{myd} (24). The Pomgnt1$_{null}$ strain used for this piece of work was generated by the Functional Glycomic Consortium (Pomgnt1$^{tm1.1Cfg}$/Mmucd) and has a deletion of exons 7–16 of the *Pomgnt1* gene. All animal experiments were carried out under license from the Home Office (UK) in accordance with the Animals (Scientific Procedures) Act 1986 and were approved by the Royal Veterinary College ethical committee. Mice were sacrificed at P0 and genotype was confirmed by polymerase chain reaction (PCR). Primers were as follows: for FKRP^{KD} mice, *Fkrp* forward: GTTGT GCTTAAACCACCTTC; *Fkrp* neo forward: GGTGGGATTAG ATAAATGCC; *Fkrp* reverse: CTAGGAGGTTGAGGATGATGG. *Fkrp* forward and *Fkrp* reverse amplified the wild-type gene, *Fkrp* neo forward and *Fkrp* reverse the mutant gene. For Pomgnt1$_{null}$ mice, primer 1607: CTGGGCCCACACAAGTCATGA; primer 1608: TCTCTGCTCAAACGCTGCCC; primer 1796: TTGAT GCTGTTATAGAGGCC. Primers 1607 and 1608 amplified the wild-type gene, primers 1607 and 1796 the mutant gene. For the Large^{myd}, primers were MydF3: ATCTCAGCTCCAAAG GGTGAAG; MydR2: GCCAATGTAAAATGAGGGGAAA; GT4F: GGCCGTGTTCCATAAGTTCAA; GT4R: GGCATACGC CTCTGTGAAAAC. MydF3 and MydR2 primers amplified the mutant gene and GT4F and GT4R the wild type.

Histology

The heads were fixed in Bouin's fixative (Sigma, Gillingham, UK) for 24 h at room temperature, before being processed and embedded in paraffin wax. Samples were serially sectioned at 5 μm, with sections collected onto charged slides (Superfrost Plus, VWR, Lutterworth, UK). At approximately 50-μm intervals, sections were stained with hematoxylin and eosin (HE). Intermediate levels were retained for immunohistochemistry.

Immunohistochemistry

Primary antibodies used in the study were as follows: rabbit anti-brain lipid binding protein (BLBP) 1:300 (raised against human BLBP, rabbit polyclonal, ABN14, Millipore, Livingston, UK), mouse anti-reelin 1:1000 (raised against recombinant fusion protein, corresponding to amino acids 164–496 of mouse reelin, monoclonal clone name G10 Abcam, Cambridge, UK) and anti-alpha DG (IIH6) 1:200 (raised against rabbit skeletal muscle membrane preparation, monoclonal, clone name IIH6C4, Millipore, Livingston, UK). Sections were deparaffinized and rehydrated. Heat-induced epitope retrieval was performed in Tris-ethylenediaminetetraacetic acid (EDTA; 10 mM Tris-HCl, 1 mM disodium EDTA, pH 8.0). All primary antibodies were diluted in phosphate buffered saline containing 0.05% Tween 20 (Sigma, Gillingham, UK) and 5% goat serum (Sigma, Gillingham, UK), and sections were incubated for 1 h at room temperature. Visualization of antibody binding used the Envision™ HRP-conjugated polymer system (Dako, Ely, UK).

Generation of brain maps

Photomicrographs of HE-stained sections were captured on a Leica DM4000B bright field microscope using a Leica DC500 camera (Leica, Milton Keynes, UK). Using Photoshop 5 (Adobe, London, UK), maps were generated to allow comparison of similar levels.

Cajal–Retzius (CR) cell counts

The number of CR cells was counted at two brain levels: the rostral cortex, at the level of the corpus callosum, and the caudal cortex, at the level of the hippocampus. To ensure consistency, levels were matched using appropriate anatomical landmarks. The number of CR cells in the cortex was counted in each section. For each mouse, three serial reelin-stained sections (5 μm apart) were counted at rostral and caudal levels, and the mean number of CR cells per section was calculated. Values were compared using a one-way analysis of variance with Dunnett's multiple comparisons.

RESULTS

Lesions within the cortex of FKRP^{KD} mice follow a rostrocaudal gradient; FKRP^{KD} mice exhibit the most severe brain phenotype and Large^{myd} mice the mildest

In FKRP^{KD}, Pomgnt1$_{null}$ and Large^{myd} mice, the rostral cortex (overlying the olfactory lobes) was disrupted. In FKRP^{KD} mice, this was characterized by a complete absence of laminar organization, with no obvious structure to the cortical plate, and apparent fusion of the interhemispheric fissure. In Pomgnt1$_{null}$ mice, as in the FKRP^{KD}, this could be indicative of non-cleavage of the prosencephalon. However, previous reports in other dystroglycanopathy models show that the hemispheres develop independently (59). In contrast to FKRP^{KD} mice, some cortical plate structure, subjacent to a substantial, disorganized, extracortical layer, was apparent in the Pomgnt1$_{null}$ mice. Large^{myd} mice at this level were phenotypically distinct—the cortical hemispheres were separate, and multifocal defects were present, with migration of neurons and glial cells into a narrow, extracortical layer (Figure 1A–D).

At the level of the corpus callosum, apparent fusion of the cortical hemispheres was still evident in FKRP^{KD} and Pomgnt1$_{null}$ mice. In both FKRP^{KD} and Pomgnt1$_{null}$ mice, disorganization was more pronounced laterally. Similar to the more rostral cortex, Large^{myd} mice exhibited focal disorganization in the cortical plate, with heterotopic neuronal and glial cells forming a narrow, subarachnoid extracortical layer (Figure 1E–H). In addition, examination of higher magnification images at this level (Figure 2) shows that normal leptomeningeal architecture is substantially disrupted in FKRP^{KD} and Pomgnt1$_{null}$ mice. In wild-type mice, the leptomeninges are readily apparent, comprising the superficial

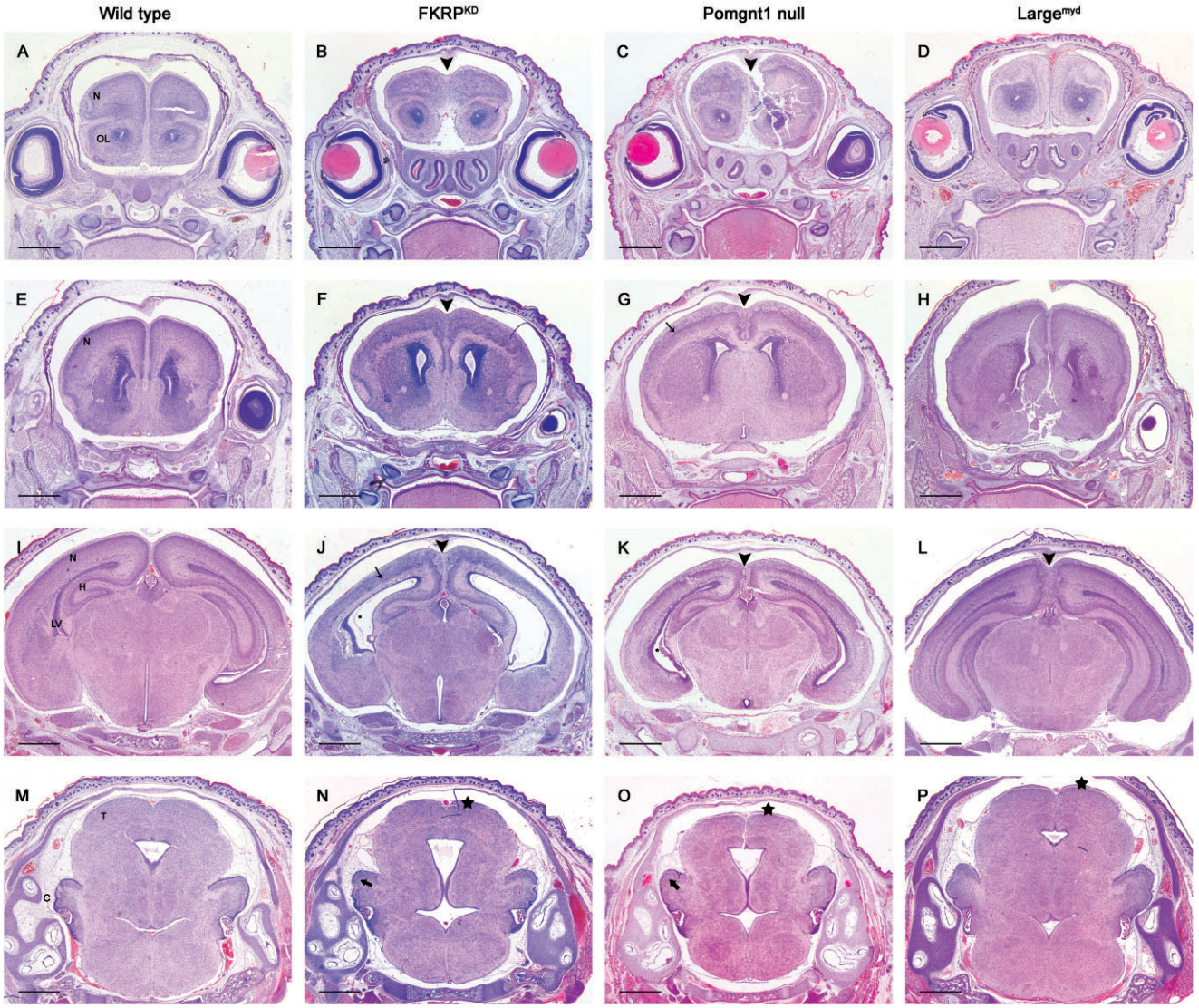

Figure 1. *There are substantial histopathological differences in the brain phenotype in FKRP^{KD}, Pomgnt1$_{null}$ and Large^{myd} mice at P0.* **A–D**. Olfactory lobes and rostral cortex. In the wild type (**A**), the organized neocortex is apparent dorsal to the olfactory lobes. In the FKRP^{KD} and Pomgnt1$_{null}$ mice (**B** and **C**, respectively), the olfactory lobes (OL) are normal, but there is fusion of the cortical hemispheres (arrowhead) and substantial dyslamination of the rostral neocortex. Cortical disorganization is most apparent in the FKRP^{KD}. In the Large^{myd} (**D**), the olfactory lobes are again normal. In these mice, the cortical hemispheres remain distinct at this level, but do exhibit disruption in lamination. **E–H**. Cortex around the level of the corpus callosum. The cortical plate is distinct, and overlain by the cell-poor marginal zone in wild-type mice (**E**). In the FKRP^{KD} (**F**), the cortex is completely disorganized, and the cortical plate is indistinct. The Pomgnt1$_{null}$ and Large^{myd} mice (**G** and **H**, respectively) have well-defined cortical plates, but these are overlain by a cell-dense, subarachnoid, extracortical layer, which is more pronounced in the Pomgnt1$_{null}$ mice. In Pomgnt1$_{null}$ mice, the lateral cortex is more disorganized than the medial cortex (fine arrow). **I–L**. Cortex around the level of the hippocampus. At this level, the FKRP^{KD}, Pomgnt1$_{null}$ and Large^{myd} mice (**J**, **K** and **L**, respectively) all exhibit incomplete formation of the interhemispheric fissure with interdigitation of neurons from opposing cortical plates. In the FKRP^{KD}, the remnants of the cortical plate are medially apparent, with dyslamination increasing laterally (**J**, fine arrow). There is ventricular dilation in the FKRP^{KD} and, to a lesser extent, in the Pomgnt1$_{null}$ (*). In addition, there is some rarefaction of the subventricular zone in the FKRP^{KD} only. **M–P**. Tectum and cerebellum. There is disorganization of the inferior colliculus, most marked in the FKRP^{KD} (star). There is some disruption to the granule cell layer of the cerebellum in the FKRP^{KD} and Pomgnt1$_{null}$ (**N** and **O**, respectively; bold arrow), when compared with the wild type (**M**). The cerebellum in the Large^{myd} (**P**) does not appear to be affected at this time point. Hematoxylin and eosin. Bars represent 400 μm. C = cerebellum; H = hippocampus; LV = lateral ventricles; N = neocortex; OL = olfactory lobes; T = tectum.

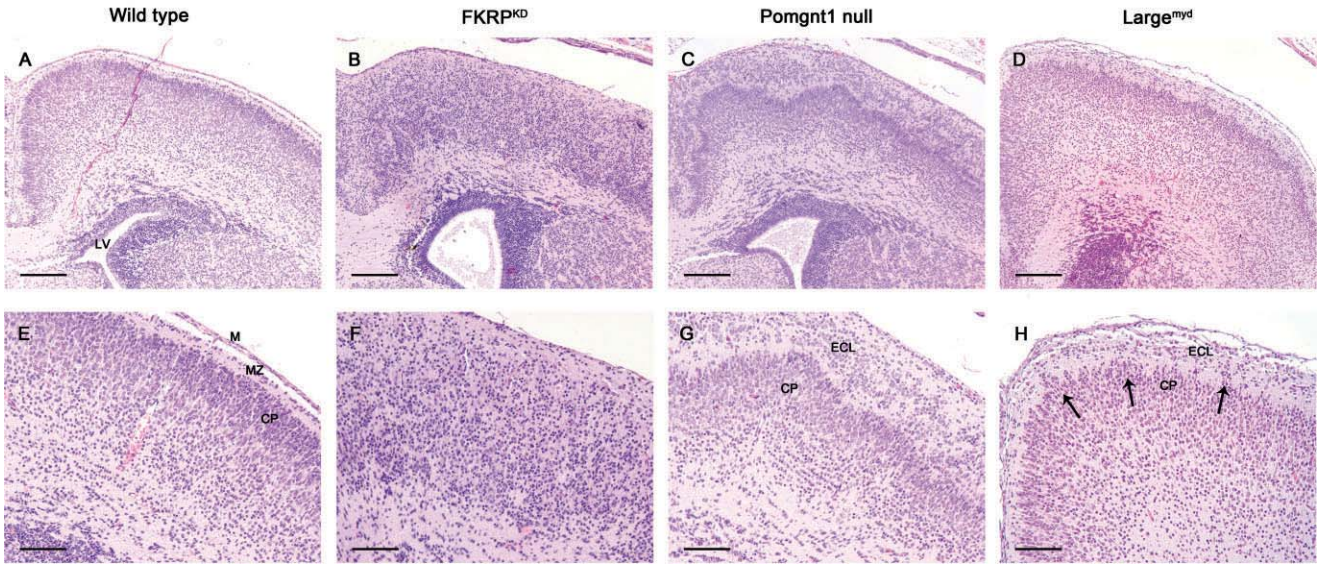

Figure 2. *Neocortex at the level of the corpus callosum*. There is consistent fusion of the cortical hemispheres in the FKRP^{KD} (**B,F**) and the Pomgnt1$_{null}$ (**C,G**), with interdigitation of neurons from opposing cortical plates. This is not consistently observed in the Large^{myd} at this level (**D,H**). The degree of disorganization of the cortical plate varies between models. The cortical plate is inapparent in FKRP^{KD} mice, and no marginal zone is observed. In Pomgnt1$_{null}$ mice, the marginal zone and cortical plate are apparent beneath a substantial extracortical layer. The Large^{myd} mice demonstrate a relatively organized cortical plate, but multifocally neurons from the cortical plate are apparent migrating through the marginal zone and the pial basement membrane and running subjacent and tangential to the arachnoid to form a narrow extracortical layer (fine arrows). The tramline appearance of the normal meninges is not present in FKRP^{KD} and Pomgnt1$_{null}$, and is only multifocally observed in Large^{myd} mice. Hematoxylin and eosin. **A–D**, bars represent 400 μm; **E–F**, bars represent 200 μm. CP = cortical plate; ECL = extracortical layer; LV = lateral ventricles; M = leptomeninges; MZ = marginal zone.

arachnoid mater, the subarachnoid space (containing the subarachnoid vessels) and the pia mater. In FKRP^{KD} and Pomgnt1$_{null}$ mice, and to a lesser degree, Large^{myd} mice, there was little, if any, distinction between these layers. The arachnoid was apparent at the cortical surface, and vessels were encompassed by heterotopic neurons and glial cells within the extracortical layer. The pia was not apparent in FKRP^{KD} and Pomgnt1$_{null}$ mice (Figure 2).

At the level of the hippocampus, in FKRP^{KD} mice the cortical plate was more established toward the midline than observed at more rostral levels of the cortex, although lateral aspects of the cortex were still extensively disrupted. In Pomgnt1$_{null}$ mice at this level, the cortex was more organized laterally. Large^{myd} mice continued to exhibit the focal defects in the cortical plate and the narrow extracortical layer present elsewhere in the cortex. Dilation of the lateral ventricles (hydrocephalus) was present in a proportion of FKRP^{KD} (3/5) and, less markedly, in Pomgnt1$_{null}$ mice (2/5) at this time point, but was not observed in Large^{myd} mice or wild-type controls (Figure 1I–L). The dentate gyrus of the hippocampus was disrupted in a subset (2/5) of FKRP^{KD} mice (Figure 3). Despite reports of disruption to the hippocampus in adult Large^{myd} and another strain of Pomgnt1$^{-/-}$ mice in the literature (33, 46), lesions were not identified in these strains at P0 in the current study.

The inferior and superior colliculi were disrupted in all three lines of mice. Lesions in Pomgnt1$_{null}$ and Large^{myd} mice were characterized by focal defects with obliteration of the subarachnoid space by heterotopic neuroglial cells. In FKRP^{KD} mice, there was some organization in the midline, but laterally, substantial defects in the pia enabled large numbers of cells to form a prominent subarachnoid layer (Figure 1M–P; Figure 4).

Subtle cerebellar lesions, characterized by disruption to the external granule cell layer, were present in 2/5 FKRP^{KD} mice and 1/5 Pomgnt1$_{null}$ mice. Cerebellar lesions were not observed in Large^{myd} mice (Figure 1M–P); however, sagittal sections may allow better assessment of cerebellar pathology.

Distinct patterns in lesion location/severity were observed; excluding the olfactory lobes of the brain, the FKRP^{KD} and Pomgnt1$_{null}$ mice showed rostrocaudal and lateromedial gradient in the severity of cortical lesions, with the greatest degree of dyslamination in the rostral and lateral aspects of the cortex. Despite the similarities in lesion localization, the brain phenotype was most substantial in FKRP^{KD} mice. Contrary to the other models, Large^{myd} mice exhibited lesions of similar character and severity throughout the cortex and midbrain (Figure 1).

Disruption to the radial glial scaffold is present in all of the mouse models of dystroglycanopathy, but the glia limitans is most extensively disrupted in FKRP^{KD} mice

In wild-type mice elongate BLBP-positive processes extended to the surface of the brain, where there was diffuse, continuous subpial staining of the radial glial end feet, which form the glia limitans (Figure 5A panels a, e, i and m).

In FKRP^{KD} mice, staining in the ventricular zone was similar to that observed in wild-type mice; however, radial glial processes were often haphazardly arranged, there was no subpial staining (complete disruption of the glia limitans) and scattered BLBP-positive foci (radial glial processes) were present within the dis-

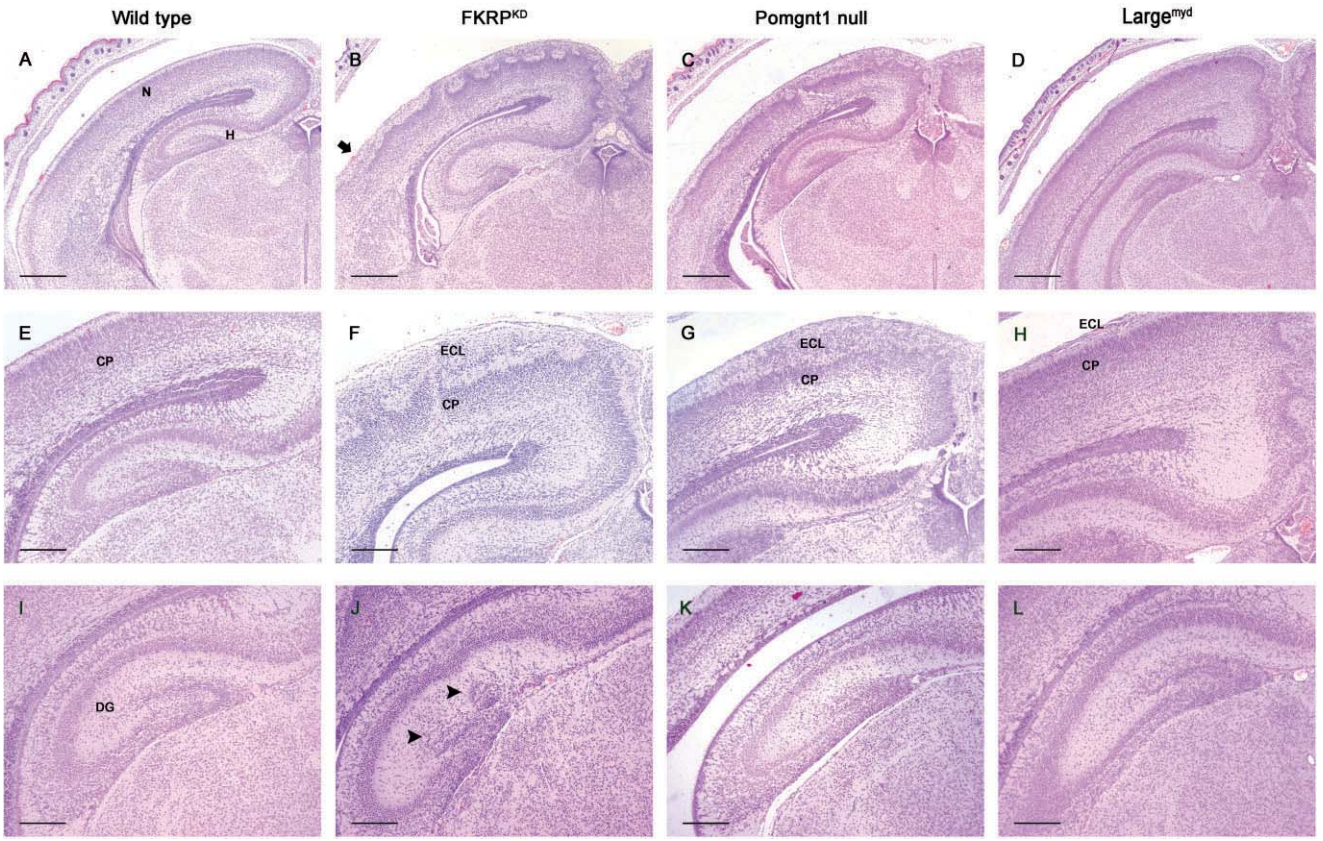

Figure 3. *Neocortex at the level of the hippocampus*. For comparison, wild-type mice are shown in **A**, **E** and **I**. In the neocortex at the level of the hippocampus, laminar architecture is most disrupted in FKRP^{KD} mice (**B, F, J**) and, to a lesser extent, Pomgnt1$_{null}$ mice (**C, G, K**). The Large^{myd} mice are least affected (**D, H, L**). Although the cortex is more organized at this level than rostrally in FKRP^{KD} mice, there is a distinct lateromedial gradient in severity of lesions (bold arrow). There is interdigitation of opposing cortical plates in all mice, including the Large^{myd} at this level. Disruption to the hippocampus, particularly the dentate gyrus, was present in a proportion of the FKRP^{KD} mice (arrowheads), but was not observed in either the Pomgnt1$_{null}$ or the Large^{myd}. Hematoxylin and eosin. **A–D**, bars represent 400 μm; **E–H**, bars represent 200 μm; **I–L**, bars represent 100 μm. CP = cortical plate; DG = dentate gyrus; ECL = extracortical layer; H = hippocampus; N = neocortex.

organized cortical plate and extracortical layer. The tectum was less affected than the cortex, but significant abnormalities were still apparent. Although relatively organized centrally and dorsomedially, discontinuous laminar staining was apparent more laterally and large numbers of heterotopic neurons and glial cells were present superficial to the glia limitans, expanding the subarachnoid space (Figure 5A panels b, f, j and n).

In Pomgnt1$_{null}$ mice, disruption to the glia limitans was still substantial, but there remained some foci of laminar staining (superficial to more organized areas of the cortical plate). In the rest of the cortex, and in the substantial extracortical layer present above these laminar foci of displaced glia limitans, were scattered BLBP-positive areas, similar to those observed in the FKRP^{KD} (radial glial processes). In the tectum, there was relatively little disruption to the laminar architecture, but multifocally, BLBP staining was discontinuous, and neuroglial cells were seen extending through the defects and expanding the subarachnoid space (Figure 5A panels c, g, k and o).

In the cortex of Large^{myd} mice, the glia limitans was largely continuous, although separated from the arachnoid by heterotopic neurons and glial cells. Multifocally there were defects in the glia limitans, which were associated with disorganization of the underlying cortical plate, and in these areas, neurons and glial cells were visibly migrating through the defects expanding the subarachnoid space and forming a narrow extracortical layer. The glia limitans in the tectum of Large^{myd} mice displayed multifocal discontinuities in BLBP staining associated with migration of neurons and glial cells into the subarachnoid space to form an extracortical layer (Figure 5A panels d, h, l and p).

These findings indicate that there are substantial differences in the degree of disruption to the glia limitans between different mouse models that correlates with the overall severity of the brain phenotype. Disruption was most pronounced in FKRP^{KD} mice and mildest in Large^{myd} mice. Pan laminin labeling to show the location of the glial limitans is shown in Figure 5B.

Expression of the IIH6 epitope of alpha DG

Expression of the IIH6 epitope of alpha DG was widespread in wild-type mice (Figure 6). In addition to intense sarcolemmal

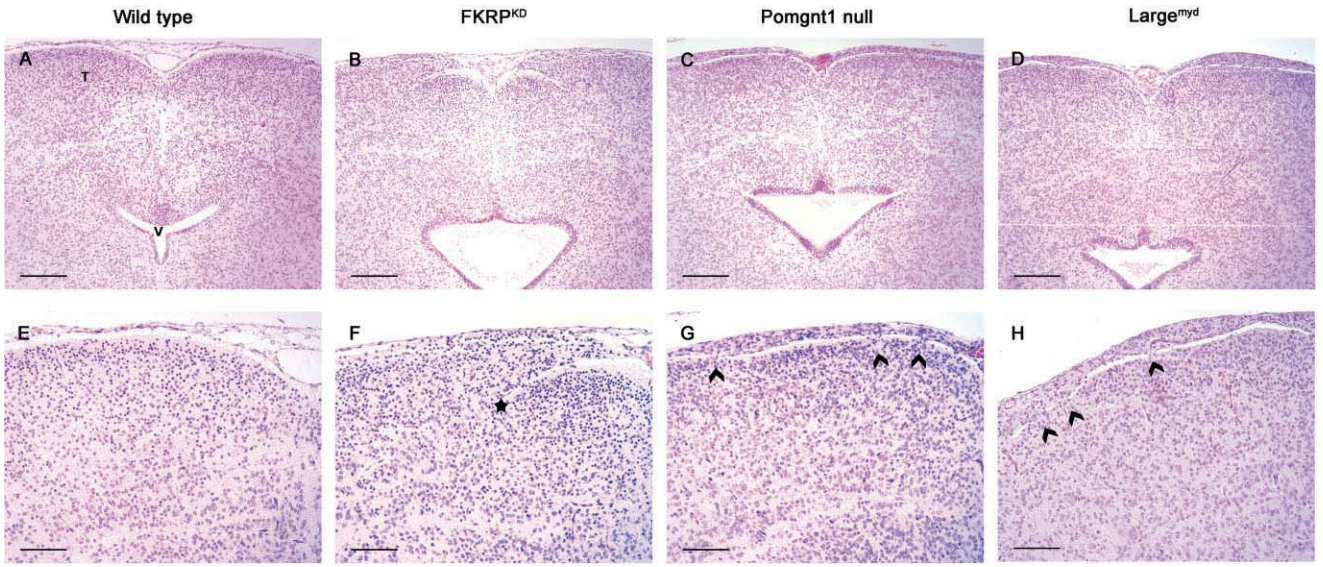

Figure 4. *Midbrain at the level of the inferior colliculus*. Midbrain: Disorganization is apparent in the superior and inferior colliculi. For comparison wild-type mice are shown in **A** and **E**. At this level, the phenotype is similar in the Pomgnt1$_{null}$ (**C,G**) and Large^{myd} mice (**D,H**), with multifocal defects in the pial basement membrane allowing migration of neuron and glial cells into the subarachnoid space (chevrons). In the FKRP^{KD} (**B,F**), there appears to be more substantial defects in the pial basement membrane laterally (star), allowing a substantial layer of neurons to form above the colliculus itself. Hematoxylin and eosin. **M–P**, bars represent 200 μm; **M–P**, bars represent 100 μm. T = tectum; V = ventricle.

staining in muscle, and fine laminar immunoreactivity at the pial basement membrane, there was intense staining of the basement membrane of blood vessels within the brain and the choroidal epithelium.

Of the dystroglycanopathy models examined, Pomgnt1$_{null}$ mice showed the most pronounced, diffuse loss of IIH6 immunoreactivity. Loss of immunoreactivity was complete and all tissues examined were immunonegative.

In FKRP^{KD} mice, a small, residual amount of sarcolemmal IIH6 immunoreactivity was observed within some, but not all, muscle groups. Immunolabeling was much less intense than that seen in wild-type mice stained concurrently. Muscle types that continue to exhibit some sarcolemmal staining included the tongue, masticatory and laryngeal muscles. Interestingly, IIH6 immunoreactivity was not observed at the sarcolemma of subcutaneous muscles or extraocular muscles. Immunolabeling of the pial basement membrane and the basement membrane of the choroidal epithelium was absent.

In Large^{myd} mice, IIH6 immunolabeling was not apparent at the pia, similar to the Pomgnt1$_{null}$ and the FKRP^{KD} mice. However, labeling of a similar distribution and intensity to that observed wild-type mice was observed at the choroidal epithelium. In addition, in Large^{myd} mice, IIH6 immunolabeling was observed in multiple other epithelial structures, including the skin, developing tooth, salivary gland, choroidal epithelium and respiratory epithelium.

Figure 5. A. Immunohistochemical evaluation of the glia limitans. **a–h**. Cortex. Brain lipid binding protein (BLBP) staining of radial glial cells and the glia limitans. The bold arrow indicates the glia limitans. In wild-type mice, the glia limitans is apparent as a continuous subpial layer (**a, e**). The glia limitans is disrupted, to varying degrees, in the FKRP^{KD}, Pomgnt1$_{null}$ and Large^{myd} (**b**, **c** and **d**, respectively). Higher power images show that in the FKRP^{KD} (**f**) mislocalized radial glial foot processes can be observed randomly scattered throughout the cortex. In Pomgnt1$_{null}$ mice (**g**), multifocal, discontinuous areas of laminar staining are present subjacent to a substantial extracortical layer. Large^{myd} mice (**h**) have a relatively well-formed glia limitans. There are multifocal small defects with migration of the neuroglial cells through the deficits into a narrow extracortical layer. Insets contained within **e**–**h** show higher power magnifications. **a–d**, bar represents 400 μm; **e–h**, bar represents 100 μm. N = neocortex; VZ = ventricular zone. **i–p**, tectum (inferior colliculus). There is disruption to the glia limitans in the midbrain of the FRKRP^{KD}, the Pomgnt1$_{null}$ and the Large^{myd} (**j**, **k** and **l**, respectively). The Pomgnt1$_{null}$ and the Large^{myd} are histologically similar at this site—there are multifocal defects in the glial limitans (fine arrows), with migration of neuroglial cells through the defects to expand the subarachnoid space (**o, p**). In addition to multifocal defects, the FKRP^{KD} exhibits disorganization laterally—laminar BLBP-positive foci (radial glial processes) are apparent toward the midline not laterally (star), and there is expansion of the subarachnoid space by a substantial population of neuroglial cells (**n**). **i–l**, bar represents 400 μm; **m–p**, bar represents 200 μm. T = tectum. **B**. Immunohistochemical staining for pan laminin in mouse models of dystroglycanopathy. **a–d**. Pan laminin staining of the cortex highlighting the location of the glia limitans (see arrow) in the wild type (**a**), FKRP^{KD} (**b**), Pomgnt1$_{null}$ (**c**) and Large^{myd} (**d**). Higher power images are shown in **e–h**. **a–d**, bar represents 200 μm; **e–h**, bar represents 100 μm.

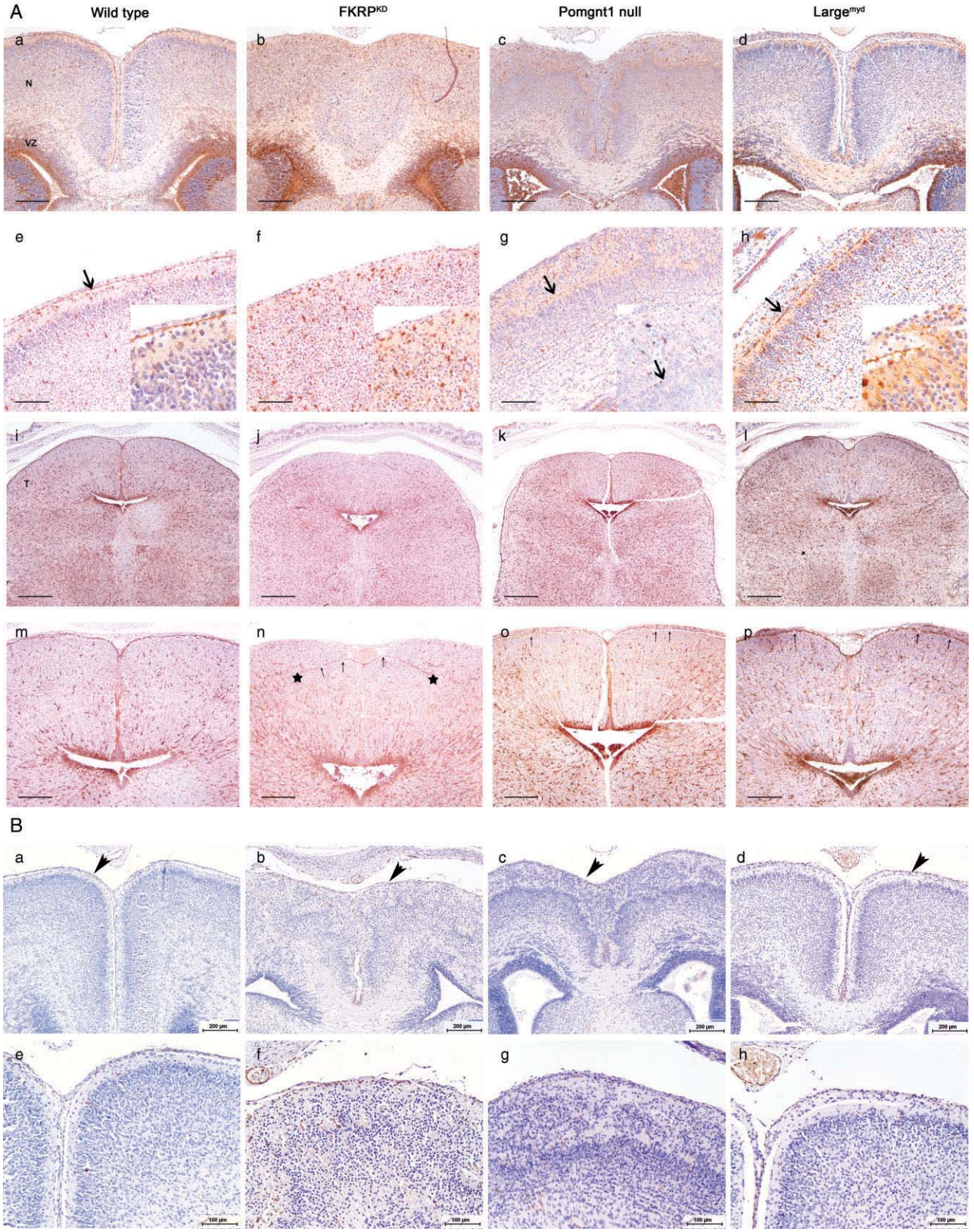

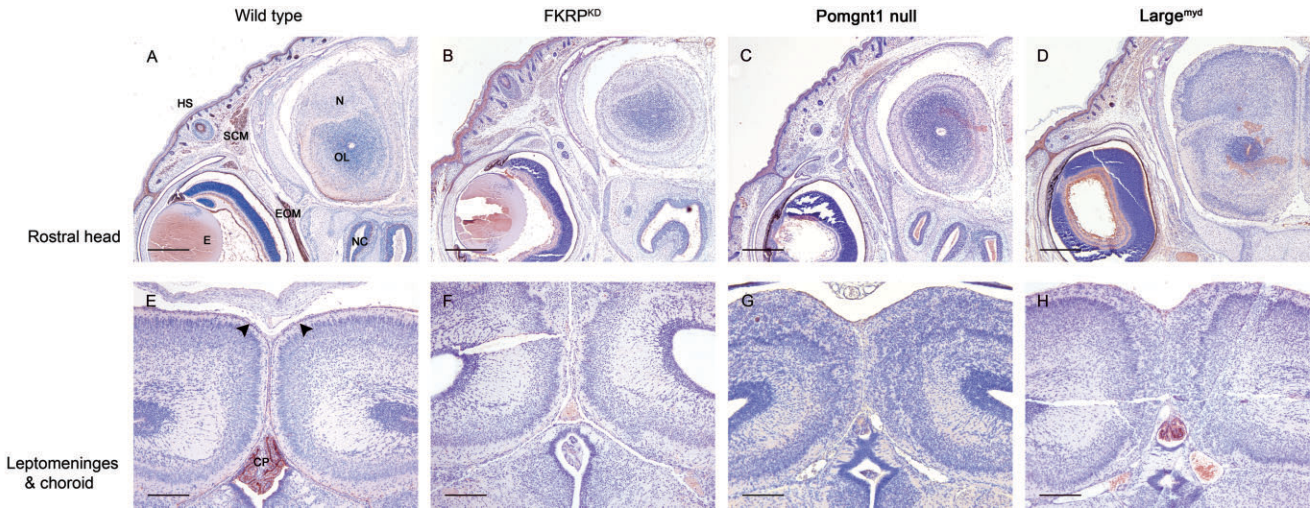

Figure 6. *Immunohistochemical staining for the IIH6 epitope of glycosylated alpha dystroglycan in mouse models of dystroglycanopathy*. **A–D**. Lateral head sections stained with IIH6 antibody. The skin, pial basement membrane and inner limiting membrane of the eye exhibit strong staining in the wild type, in addition to sarcolemmal staining present in the extraocular and subcutaneous muscles (**A**). Staining of all of these structures is absent in FKRP^{KD} and Pomgnt1$_{null}$ mice (**B, C**). In Large^{myd} mice (**D**), the skin remains immunopositive, but staining is absent in other tissues. Bars represent 400 μm. **E–H**. IIH6 staining in the brain at the level of the hippocampus. In the WT (**E**), the basement membrane of choroid plexus is strongly immunopositive and there is a narrow, laminar staining pattern at the pial basement membrane (arrowheads). In the FKRP^{KD} and Pomgnt1$_{null}$ mice (**F** and **G**, respectively), no staining is apparent. In the Large^{myd}, the basement membrane of the choroid plexus is strongly immunopositive, but there is no staining at the pial basement membrane. Bars represent 200 μm. CP = choroid plexus; E = eye; EOM = extraocular muscle; HS = haired skin; N = neocortex; NC = nasal cavity; OL = olfactory lobe; SCM = subcutaneous muscle.

Mislocalization of CR cells in mouse models of dystroglycanopathy

CR cells arise early in brain development and are key to the ordered migration of neurons within the cortex. They produce reelin—an extracellular glycoprotein that has roles in neuronal migration, radial glial differentiation and providing a "stop signal" to prevent overmigration of neurons (53).

In wild-type mice, CR cells were present multifocally within the superficial molecular layer, orientated parallel to the surface. However, in FKRP^{KD} mice the majority of CR cells were located around the anterior cerebral artery. Scattered CR cells were present within the disorganized cortical plate. Only rarely were CR cells apparent in more lateral aspects of the cortex. In Pomgnt1$_{null}$ mice, there was still some clustering of CR cells around the anterior cerebral artery, but a larger proportion of cells extended away from the midline, although they were still organized randomly and within the extracortical layer. In Large^{myd} mice, CR cell localization was more orderly, and although often CR cells were present within the extracortical layer, they assumed the tangential orientation and the discontinuous, laminar staining pattern of the wild type in some areas (Figure 7A–H).

Cell counts identified a statistically significant decrease in the number of CR cells in the rostral cortex (level of the corpus callosum) in FKRP^{KD} and Pomgnt1$_{null}$ mice ($P = 0.0002$ and $P = 0.0017$, respectively). In FKRP^{KD} mice, there was a concurrent, statistically significant ($P = 0.046$) increase in the number of CR cells at the level of the hippocampus. In Large^{myd} mice, there was no difference in the number of CR cells (when compared with wild-type mice) at either level (Figure 7I,J). These findings may suggest either a local (failure of migration) or total (failure of differentiation/increased loss) decrease in the number of CR cells in the cortex.

DISCUSSION

FKRP, POMGNT1 and LARGE are demonstrated or putative glycosyltransferases involved in the post-translational modification of alpha DG (6, 9, 11, 24, 49, 78, 86). They are located within the Golgi apparatus, and are hypothesized to work sequentially, with each involved in the addition of a separate sugar moiety (10, 20, 37, 41, 86). They represent 3 of the 18 genes currently implicated in the dystroglycanopathies, mutations in which result in the hypoglycosylation of alpha DG (4, 5, 9, 12, 13, 43, 44, 49, 50, 65, 72, 77–80, 82, 83, 86, 87). At the severe end of the dystroglycanopathy spectrum (WWS and MEB), patients exhibit substantial structural brain abnormalities, including neuronal migration defects (manifest as pachygyria or cobblestone lissencephaly), hydrocephalus and cerebellar defects (17).

FKRP^{KD} and Pomgnt1$_{null}$ brain lesions exhibit a rostrocaudal and mediolateral gradient in severity

There was a substantial variation in brain phenotype between the FKRP^{KD}, Pomgnt1$_{null}$ and Large^{myd} models, to the degree that the models could be distinguished based on morphology alone. This is consistent with reports from Devisme *et al* (15), who found that

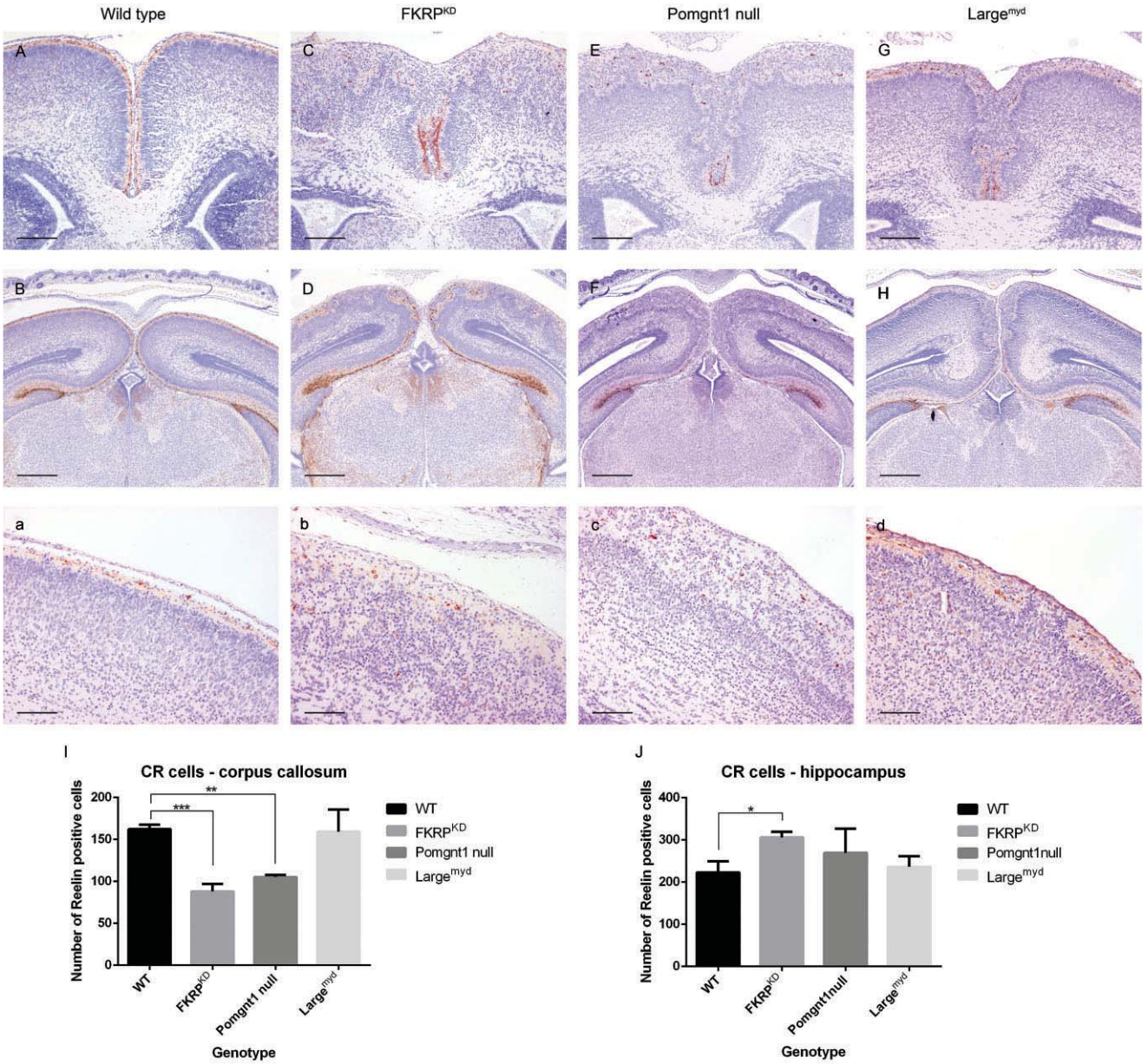

Figure 7. *Mislocalization of the Cajal–Retzius (CR) cells*. Immunohistochemical staining of the CR cells with an antibody to reelin, at the level of the corpus callosum (**A, C, E, G**, bar represents 200 μm) and at the hippocampus (**B, D, F, H**, bar represents 400 μm). In wild-type mice, there are multifocal, tangentially orientated, reelin-positive CR cells that form an intermittent, single-cell layer within the marginal zone (**A, B**). Large numbers of CR cells are present at the hippocampus. In FKRP^{KD} mice, there is a significant decrease in the number of reelin-positive cells at the level of the corpus callosum (**C**). Those present are disorganized, haphazardly orientated and predominantly clustered around the anterior cerebral artery. At the level of the hippocampus, more normally distributed and orientated CR cells appear to be associated with more ordered areas of the cortical plate (**D**). In the Pomgnt1$_{null}$ mice (**E**), there is less clustering of the CR cells around the anterior cerebral artery. CR cells extend further laterally, although are randomly distributed within the extracortical layer. Again, CR cell distribution appears more normal at the level of the hippocampus (**F**). In the Large^{myd} (**G**), CR cells are orientated predominantly transversely (as in the wild type) but are overlain by a narrow extracortical layer, rostrally. There is some disruption in the midline at the level of the hippocampus, in areas of fusion of opposing cortical plates (**H**). **a–d**. Higher magnification views of the cortex at the level of the corpus callosum, lateral to the interhemispheric fissure (bars represent 100 μm). At the level of the corpus callosum (**I**), there is a statistically significant decrease in the number of CR cells in FKRPKD ($P = 0.0002$) and Pomgnt1$_{null}$ mice ($P = 0.0017$) relative to wild-type mice (one-way analysis of variance with Dunnett's multiple comparisons). This is not observed in Large^{myd} mice ($P = 0.986$). At the level of the hippocampus (**J**) in FKRPKD, there is a statistically significant increase in the number of CR cells relative to wild type ($P = 0.046$) but no statistically significant differences in the number of CR cells in either Pomgnt1$_{null}$ or Large^{myd} mice relative to wild type ($P = 0.304$ and $P = 0.930$, respectively).

morphological classification of neuropathologic findings in fetuses with cobblestone lissencephaly enabled accurate orientation of genetic screening, and indicating that the mouse models largely provide a good representation of the human disease (15).

Mice from all strains exhibited distinct patterns of lesions within the brain, which varied according to the mutation. $FKRP^{KD}$ and $Pomgnt1_{null}$ mice exhibited a rostrocaudal gradient in the severity of brain lesions, with lesions most pronounced in the rostral cortex and progressively milder more caudally. Additionally, there were differences mediolaterally, with cortical organization greatest toward the midline, and disruption extending laterally. Unlike the other models examined, $Large^{myd}$ mice did not exhibit this gradient of lesions—defects in the $Large^{myd}$ were multifocal and present throughout the brain.

Although a gradient of lesion severity has not been previously reported cases of cobblestone lissencephaly in patients, specific lesion localization is reported in other human neuronal migration defects. Loss of function mutations in the G-protein coupled receptor 56 in patients is associated with the autosomal recessive brain abnormality bilateral frontoparietal polymicrogyria (BFFP), in which a neuronal migration defect is isolated to the frontal and parietal lobes of the brain (14). A gradient of lesions is also observed in cases of classical lissencephaly. *LIS1* mutations produce lesions that are more severe in the occipital lobe (posterior-predominant), whereas those produced by *DCX1* mutations are more severe in the frontal lobes (anterior-predominant) (62, 66). The mechanisms underlying the specific lesion localization in BFFP or classical lissencephaly are unknown, although in the case of classical lissencephaly is it is believed to be due to Dcx and Lis1 having distinct, but related roles in signal transduction pathways (62).

Previously, there has been the suggestion of a mediolateral gradient in lesion severity in conditional DG null mice that corresponds to the time point at which DG is lost (69). In Nestin cre-DG null mice, where there is deletion of DG from around E10.5, loss of lamination and neuroglial heterotopia extend to the lateral cortex and pyriform lobe, whereas in GFAP cre-DG null mice, in which DG is deleted around E13.5, lesions are focal and present only in the medial cortex (69). The differences in lesion gradient observed in $FKRP^{KD}$, $Pomgnt1_{null}$ and $Large^{myd}$ mice may therefore represent temporal differences in the requirement for these proteins, or in the case of the $Large^{myd}$, may suggest the ability of Large homolog Large2 to compensate for the loss of Large early in development. The latter point is of particular relevance as in this work, immunolabeling for the IIH6 epitope of alpha DG revealed continued expression of glycosylated alpha DG in the choroid plexus of this model.

The degree of CR cell disruption is correlated with the severity of the brain lesions

In $FKRP^{KD}$, $Pomgnt1_{null}$ and $Large^{myd}$ mice, the rostrocaudal and mediolateral gradient of brain lesions correlates with the degree of CR cell disruption observed in each of the mouse strains. The areas of the cortex with the most substantial dyslamination are those with the lowest number of CR cells (Figure 7). $FKRP^{KD}$ mice, which exhibit the most substantial mislocalization of CR cells, also have the most pronounced gradient of lesions, whereas in $Large^{myd}$ mice, which have minimal CR cell mislocalization, a gradient is not apparent. CR cells are one of the earliest cell populations produced in the developing brain, arising from the caudomedial pallium (primarily the cortical hem) and undergoing tangential migration to occupy the marginal zone of the entire cortex (51, 52).

Reelin is an extracellular glycoprotein produced by the CR cells, and this protein has a number of critical roles in brain development. Reeler mice carry a mutation in the *Reln* gene that encodes reelin. These mice exhibit marked cortical disruption, disorganization and inversion of cell layers, with substantial malformation of the radial glial scaffold, and patients with mutations in *RELN* exhibit pachygyria with severe cerebellar hypoplasia, phenotypically similar to the lesions seen in patients with WWS and MEB (27, 34, 81). It has been demonstrated that reelin induces a radial glial phenotype in neuroepithelial progenitors via activation of Notch-1 (40), and it arrests neuronal migration and promotes normal cortical lamination by providing a stop signal through the binding of $\alpha_3\beta_1$ integrin (18, 47). Reelin is also responsible for the regulation of radial glial cells—in the Emx1/2 and p73 knockout mice, where there is premature loss of CR cells, and in animals where the CR cells have been chemically ablated, there are decreased numbers of radial glial cells and premature transformation of radial glial cells into astrocytes (54, 70, 74).

The severity of disruption to the radial glial scaffold is associated with CR cell mislocalization

BLBP is expressed by radial glial cells. It is a cytoplasmic protein involved in fatty acid uptake, transport and metabolism (21). BLBP expression, and the radial glial phenotype, is induced in neuroepithelial progenitors via reelin-mediated activation of Notch-1 (40). Radial glial cells are bipolar cells with elongated processes that extend from the ventricular zone to the pial basement membrane, spanning the developing cortex. This provides a scaffold along which neurons migrate—an integral component of the "inside out" development of the mammalian cortex (63). In addition, radial glial cells provide a progenitor population (28, 60, 76). Radial glial foot processes form the glia limitans (the glial limiting membrane) in the developing brain, and as such form part of the blood–brain barrier (63). Defects in the radial glial scaffold, either physical, chemical or genetic, produce substantial abnormalities in neuronal migration and layering, causing neuronal migration defects and cobblestone lissencephaly, and recapitulate the brain lesions seen in patients with WWS and MEB caused by mutations in *FKRP*, *POMGNT1* and *LARGE* (60, 61, 64).

In $FKRP^{KD}$, $Pomgnt1_{null}$ and $Large^{myd}$ mice at P0, there was disruption to the radial glial end feet (glia limitans), most extensive in the $FKRP^{KD}$, which was characterized by alterations in the pattern and distribution of BLBP staining. This, alongside cortical dysplasia with obliteration of the subarachnoid space, neuroglial heterotopia and the apparent fusion of the interhemispheric fissure, indicate that radial glial cells are substantially disrupted in all of the examined models of dystroglycanopathy, but most notably in the $FKRP^{KD}$. Again, the areas of most substantial disruption to glial scaffold were those with the lowest number of CR cells. Although in humans additional defects in the subpial granular layer originally described by Brun may contribute to these

alterations, this layer was not examined in this study as it is much more developed in human than other mammals (23).

$FKRP^{KD}$, $Pomgnt1_{null}$ and $Large^{myd}$ mice all exhibit mislocalization of CR cells; however, the relative decrease in the number of CR cells in the rostral cortex, with the concurrent increase in the area of the hippocampus in $FKRP^{KD}$ and $Pomgnt1_{null}$ mice, suggests that there is failure of tangential migration of CR cells in these models. This is in marked contrast to the brain lesions observed in $Large^{myd}$ mice.

Given the role CR cells and reelin play in neuronal migration and the organization of the radial glia, and the correlation between the degree of CR cell mislocalization and the location and severity of the brain lesions observed, this suggests that CR cell mislocalization may have a significant role in the manifestation of the brain phenotype. In addition, it suggests that factors affecting CR cell migration may underpin the pathogenesis of the structural brain defects in $FKRP^{KD}$ and $Pomgnt1_{null}$ mice, but not $Large^{myd}$ mice. Radial glial fibers form the initial migratory microcolumns, whereas the migration of inhibitory interneurons initiated prior to radial migration forms the marginal zone of the preplate that includes CR cells, molecular zone and subplate neurons (67). Horizontal lamination in the newborn $FKRP^{KD}$ brain as detected using markers such as Tbr1 and Ctip2 is clearly evident, although it shows a disturbed pattern (2).

Previously, it has been hypothesized that disruption to the glia limitans and neuronal migration defects are largely localized to the areas of the brain which undergo most pronounced and rapid expansion during development. In agreement with this, the brain lesions in dystroglycanopathy models were reported to develop due to failure of the radial glial cells to appropriately organize the basement membrane during periods of rapid cortical expansion (59). This idea was strengthened by data from a $Pomgnt1^{-/-}$ strain, whereby the basement membrane was initially normal and was intact at E11.5, but abnormalities were apparent by E13.5 (35). Similarly, in Nestin cre-DG null mice, in which DG was knocked out from E10.5, abnormalities in the basement membrane were first apparent at E13.5 (69).

Radial glial end feet retraction could potentially account for the lesions observed in $Large^{myd}$ mice, in which CR cells are mislocalized but do not exhibit a failure of migration. However, our observations of a disruption in CR cell migration in $FKRP^{KD}$ and $Pomgnt1_{null}$ mice are suggestive of a more complex pathogenesis albeit not one that excludes a role for the radial glia. Indeed previous work in which the radial glial scaffold was disrupted without impacting on either the meninges or basement membrane integrity demonstrated a primary role for radial glia in Cajal-Retzius cell localization (42).

The mechanisms involved in the migration of CR cells from their birthplace to cover the marginal zone of the entire cortex are not fully understood, although the process is known to be influenced by a number of factors. The leptomeninges are central to the orchestration of this process, through both their physical presence and through chemokine signaling via the CXCL12/CXCR4 pathway (7). Surgical, chemical or genetic disruption of the leptomeninges produces CR cell degeneration with pronounced disruption in CR cell localization, further indicating the importance of the leptomeninges to CR cells (29, 39, 47, 74, 75). In addition, the leptomeninges are morphologically abnormal in the mouse models of dystroglycanopathy, as identified in this study and in a $Pomgnt1^{-/-}$ mouse model in work by Yang *et al* (84). Taken together, this implicates a role for abnormalities in leptomeningeal cells in the pathogenesis of the dystroglycanopathies.

Expression of the IIH6 epitope of alpha DG varies between mouse models of dystroglycanopathy

Despite the presence of significant brain phenotypes in $FKRP^{KD}$, $Pomgnt1_{null}$ and $Large^{myd}$ mice, and published muscle and eye phenotypes in these models (1, 2, 31, 33), there was significant variation in the expression of the glycoepitope of alpha DG recognized by the IIH6 antibody between them. In both $FKRP^{KD}$ and $Pomgnt1_{null}$ mice, no IIH6 immunolabeling was identified in the brain.

In the brain of $Large^{myd}$ mice, the IIH6 epitope was still strongly expressed at the choroid plexus, despite an absence of IIH6 expression at the pia mater, and at the sarcolemma in the muscle. In addition, in $Large^{myd}$ mice, IIH6 continued to be expressed throughout epithelial structures. *In situ* hybridization data provided by Hewitt (pers. comm.) identified expression of the *Large* paralog *Large2* in the choroid plexus and in epithelial structures outside of the brain. *Large2* has been identified as having the same xylosyltransferase and glucuronyltransferase activities as *Large*, but with different biochemical properties, most likely accounting for the difference in tissue expression observed by Grewal *et al* (3, 25, 38). Interestingly, despite the identification of *Large2* expression at the choroid plexus by *in situ* hybridization, expression was not observed in the brain with reverse transcription-PCR (RT-PCR), northern blot or dot blot analysis (25). The reason for the discrepancy between these results is not certain, but may relate to the expression of *Large2* by a very limited population of cells being "diluted" in the whole brain homogenates used for RT-PCR, northern blot and dot blots. Other than the labeling at the choroid plexus, the expression of the IIH6 epitope of alpha DG appeared to correlate with the expression patterns reported by Grewal *et al* (25), and was observed exclusively within epithelial structures.

It is not known how the retention of expression of glycosylated alpha DG in the choroid plexus relates to the relatively mild brain phenotype observed in $Large^{myd}$ mice. Studies of embryonic development in $Large^{myd}$ mice have not been published; therefore, it is not known whether the deficiency in *Large* is compensated for by the upregulation of *Large2* at earlier developmental time points.

This work clearly demonstrates that there is substantial variation in the brain phenotype between mouse models of the dystroglycanopathies, indicating that a "one-model-fits-all" approach to the investigation of underlying mechanisms is not appropriate, and reiterating the importance of both careful model selection and the use of multiple mouse models, in investigative work. Because CR cells typically respond to cues originating from the meninges, our results suggest that although cortical defects in $Large^{myd}$ mice are consistent with a disturbance of the radial glial scaffold as previously reported, the more severe phenotype observed in $FKRP^{KD}$ and $Pomgnt1_{null}$ mice imply additional defects in the meninges. Although the subplate was not included in the present study, it is composed of early born neurons that are of substantial interest to the present work in that they are generated around the same time as the CR cells. Indeed, the subplate is a highly dynamic structure the transcriptomic profile of which

suggests a number of intriguing roles that change through development. Future work in this area might profit from an analysis of this heterogenous cell population (32).

It should be noted that although the present paper focuses on the role of the pial basement membrane in cortical development, neuron : neuron and neuron : glial interactions also play a key role in orchestrating development of the cortex. These interactions are mediated by integrins, N-cadherin, gap junction proteins together with a number of signaling pathways, some of which are downstream of reelin (71). Future work may benefit particularly from a more detailed exploration of adhesion receptor trafficking that underlies the migration of all cells and laminin internalization in the secondary dystroglycanopathies, the latter of which has been shown to utilize DG in cancer cells (45).

In summary our observations implicate gene-specific differences in the pathogenesis of brain lesions in this group of disorders. Further work is required to identify whether a defect in another cell type (such as the leptomeningeal cells) contributes to these phenotypes.

ACKNOWLEDGMENTS

HSB and SCB designed the study and wrote the paper. HSB, JLW and MH performed the experiments and analyzed the data. SCB gratefully acknowledges the support of the Muscular Dystrophy Association (USA) and Association contres les myopathies (AFM). HSB is supported by the Royal Veterinary College.

CONFLICT OF INTEREST

The authors confirm that they have no conflict of interests either personally or financially.

REFERENCES

1. Ackroyd MR, Skordis L, Kaluarachchi M, Godwin J, Prior S, Fidanboylu M *et al* (2009) Reduced expression of fukutin related protein in mice results in a model for fukutin related protein associated muscular dystrophies. *Brain* **132** (Pt 2):439–451.
2. Ackroyd MR, Whitmore C, Prior S, Kaluarachchi M, Nikolic M, Mayer U *et al* (2011) Fukutin-related protein alters the deposition of laminin in the eye and brain. *J Neurosci* **31**:12927–12935.
3. Ashikov A, Buettner FF, Tiemann B, Gerardy-Schahn R, Bakker H (2013) LARGE2 generates the same xylose- and glucuronic acid-containing glycan structures as LARGE. *Glycobiology* **23**:303–309.
4. Barone R, Aiello C, Race V, Morava E, Foulquier F, Riemersma M *et al* (2012) DPM2-CDG: a muscular dystrophy-dystroglycanopathy syndrome with severe epilepsy. *Ann Neurol* **72**:550–558.
5. Beltran-Valero de Bernabe D, Currier S, Steinbrecher A, Celli J, van Beusekom E, van der Zwaag B *et al* (2002) Mutations in the O-mannosyltransferase gene POMT1 give rise to the severe neuronal migration disorder Walker-Warburg syndrome. *Am J Hum Genet* **71**:1033–1043.
6. Beltran-Valero de Bernabe D, Voit T, Longman C, Steinbrecher A, Straub V, Yuva Y *et al* (2004) Mutations in the FKRP gene can cause muscle-eye-brain disease and Walker-Warburg syndrome. *J Med Genet* **41**:e61.
7. Borrell V, Marin O (2006) Meninges control tangential migration of hem-derived Cajal-Retzius cells via CXCL12/CXCR4 signaling. *Nat Neurosci* **9**:1284–1293.
8. Bouchet C, Gonzales M, Vuillaumier-Barrot S, Devisme L, Lebizec C, Alanio E *et al* (2007) Molecular heterogeneity in fetal forms of type II lissencephaly. *Hum Mutat* **28**:1020–1027.
9. Brockington M, Blake DJ, Prandini P, Brown SC, Torelli S, Benson MA *et al* (2001) Mutations in the fukutin-related protein gene (FKRP) cause a form of congenital muscular dystrophy with secondary laminin alpha2 deficiency and abnormal glycosylation of alpha-dystroglycan. *Am J Hum Genet* **69**:1198–1209.
10. Brockington M, Torelli S, Prandini P, Boito C, Dolatshad NF, Longman C *et al* (2005) Localization and functional analysis of the LARGE family of glycosyltransferases: significance for muscular dystrophy. *Hum Mol Genet* **14**:657–665.
11. Brockington M, Yuva Y, Prandini P, Brown SC, Torelli S, Benson MA *et al* (2001) Mutations in the fukutin-related protein gene (FKRP) identify limb girdle muscular dystrophy 2I as a milder allelic variant of congenital muscular dystrophy MDC1C. *Hum Mol Genet* **10**:2851–2859.
12. Buysse K, Riemersma M, Powell G, van Reeuwijk J, Chitayat D, Roscioli T *et al* (2013) Missense mutations in beta-1,3-N-acetylglucosaminyltransferase 1 (B3GNT1) cause Walker-Warburg syndrome. *Hum Mol Genet* **22**: 1746–1754.
13. Carss KJ, Stevens E, Foley AR, Cirak S, Riemersma M, Torelli S *et al* (2013) Mutations in GDP-mannose pyrophosphorylase B cause congenital and limb-girdle muscular dystrophies associated with hypoglycosylation of alpha-dystroglycan. *Am J Hum Genet* **93**:29–41.
14. Chiang NY, Hsiao CC, Huang YS, Chen HY, Hsieh IJ, Chang GW, Lin HH (2011) Disease-associated GPR56 mutations cause bilateral frontoparietal polymicrogyria via multiple mechanisms. *J Biol Chem* **286**:14215–14225.
15. Devisme L, Bouchet C, Gonzales M, Alanio E, Bazin A, Bessieres B *et al* (2012) Cobblestone lissencephaly: neuropathological subtypes and correlations with genes of dystroglycanopathies. *Brain* **135** (Pt 2):469–482.
16. Dobyns WB, Kirkpatrick JB, Hittner HM, Roberts RM, Kretzer FL (1985) Syndromes with lissencephaly. II: Walker-Warburg and cerebro-oculo-muscular syndromes and a new syndrome with type II lissencephaly. *Am J Med Genet* **22**:157–195.
17. Dobyns WB, Pagon RA, Armstrong D, Curry CJ, Greenberg F, Grix A *et al* (1989) Diagnostic criteria for Walker-Warburg syndrome. *Am J Med Genet* **32**:195–210.
18. Dulabon L, Olson EC, Taglienti MG, Eisenhuth S, McGrath B, Walsh CA *et al* (2000) Reelin binds alpha3beta1 integrin and inhibits neuronal migration. *Neuron* **27**:33–44.
19. Ervasti JM, Campbell KP (1993) A role for the dystrophin-glycoprotein complex as a transmembrane linker between laminin and actin. *J Cell Biol* **122**:809–823.
20. Esapa CT, Benson MA, Schroder JE, Martin-Rendon E, Brockington M, Brown SC *et al* (2002) Functional requirements for fukutin-related protein in the Golgi apparatus. *Hum Mol Genet* **11**:3319–3331.
21. Feng L, Hatten ME, Heintz N (1994) Brain lipid-binding protein (BLBP): a novel signaling system in the developing mammalian CNS. *Neuron* **12**:895–908.
22. Gee SH, Montanaro F, Lindenbaum MH, Carbonetto S (1994) Dystroglycan-alpha, a dystrophin-associated glycoprotein, is a functional agrin receptor. *Cell* **77**:675–686.
23. Goffinet AM (2006) What makes us human? A biased view from the perspective of comparative embryology and mouse genetics. *J Biomed Discov Collab* **1**:16.
24. Grewal PK, Hewitt JE (2002) Mutation of large, which encodes a putative glycosyltransferase, in an animal model of muscular dystrophy. *Biochim Biophys Acta* **1573**:216–224.

25. Grewal PK, McLaughlan JM, Moore CJ, Browning CA, Hewitt JE (2005) Characterization of the LARGE family of putative glycosyltransferases associated with dystroglycanopathies. *Glycobiology* **15**:912–923.
26. Hara Y, Balci-Hayta B, Yoshida-Moriguchi T, Kanagawa M, Beltran-Valero de Bernabe D, Gundesli H *et al* (2011) A dystroglycan mutation associated with limb-girdle muscular dystrophy. *N Engl J Med* **364**:939–946.
27. Hartfuss E, Förster E, Bock HH, Hack MA, Leprince P, Luque JM *et al* (2003) Reelin signaling directly affects radial glia morphology and biochemical maturation. *Development* **130**:597–4609.
28. Hartfuss E, Galli R, Heins N, Gotz M (2001) Characterization of CNS precursor subtypes and radial glia. *Dev Biol* **229**:15–30.
29. Hecht JH, Siegenthaler JA, Patterson KP, Pleasure SJ (2010) Primary cellular meningeal defects cause neocortical dysplasia and dyslamination. *Ann Neurol* **68**:454–464.
30. Henry MD, Campbell KP (1998) A role for dystroglycan in basement membrane assembly. *Cell* **95**:859–870.
31. Hewitt JE (2010) Investigating the functions of LARGE: lessons from mutant mice. *Methods Enzymol* **479**:367–381.
32. Hoerder-Suabedissen A, Molnar Z (2015) Development, evolution and pathology of neocortical subplate neurons. *Nat Rev Neurosci* **16**:133–146.
33. Holzfeind PJ, Grewal PK, Reitsamer HA, Kechvar J, Lassmann H, Hoeger H *et al* (2002) Skeletal, cardiac and tongue muscle pathology, defective retinal transmission, and neuronal migration defects in the Large^{myd} mouse defines a natural model for glycosylation-deficient muscle–eye–brain disorders. *Hum Mol Genet* **11**:2673–2687.
34. Hong SE, Shugart YY, Huang DT, Shahwan SA, Grant PE, Hourihane JO *et al* (2000) Autosomal recessive lissencephaly with cerebellar hypoplasia is associated with human RELN mutations. *Nat Genet* **26**:93–96.
35. Hu H, Yang Y, Eade A, Xiong YF, Qi Y (2007) Breaches of the pial basement membrane and disappearance of the glia limitans during development underlie the cortical lamination defect in the mouse model of muscle-eye-brain disease. *J Comp Neurol* **501**:168–183.
36. Ibraghimov-Beskrovnaya O, Ervasti JM, Leveille CJ, Slaughter CA, Sernett SW, Campbell KP (1992) Primary structure of dystrophin-associated glycoproteins linking dystrophin to the extracellular matrix. *Nature* **355**:696–702.
37. Inamori K, Yoshida-Moriguchi T, Hara Y, Anderson ME, Yu L, Campbell KP (2012) Dystroglycan function requires xylosyl- and glucuronyltransferase activities of LARGE. *Science* **335**:93–96.
38. Inamori KI, Hara Y, Willer T, Anderson ME, Zhu Z, Yoshida-Moriguchi T, Campbell KP (2013) Xylosyl- and glucuronyltransferase functions of LARGE in alpha-dystroglycan modification are conserved in LARGE2. *Glycobiology* **23**:295–302.
39. Inoue T, Ogawa M, Mikoshiba K, Aruga J (2008) Zic deficiency in the cortical marginal zone and meninges results in cortical lamination defects resembling those in type II lissencephaly. *J Neurosci* **28**:4712–4725.
40. Keilani S, Sugaya K (2008) Reelin induces a radial glial phenotype in human neural progenitor cells by activation of Notch-1. *BMC Dev Biol* **8**:69.
41. Keramaris-Vrantsis E, Lu PJ, Doran T, Zillmer A, Ashar J, Esapa CT *et al* (2007) Fukutin-related protein localizes to the Golgi apparatus and mutations lead to mislocalization in muscle *in vivo*. *Muscle Nerve* **36**:455–465.
42. Kwon HJ, Ma S, Huang Z (2011) Radial glia regulate Cajal-Retzius cell positioning in the early embryonic cerebral cortex. *Dev Biol* **351**:25–34.
43. Lefeber DJ, de Brouwer AP, Morava E, Riemersma M, Schuurs-Hoeijmakers JH, Absmanner B *et al* (2011) Autosomal recessive dilated cardiomyopathy due to DOLK mutations results from abnormal dystroglycan O-mannosylation. *PLoS Genet* **7**:e1002427.
44. Lefeber DJ, Schonberger J, Morava E, Guillard M, Huyben KM, Verrijp K *et al* (2009) Deficiency of Dol-P-Man synthase subunit DPM3 bridges the congenital disorders of glycosylation with the dystroglycanopathies. *Am J Hum Genet* **85**:76–86.
45. Leonoudakis D, Huang G, Akhavan A, Fata JE, Singh M, Gray JW, Muschler JL (2014) Endocytic trafficking of laminin is controlled by dystroglycan and is disrupted in cancers. *J Cell Sci* **127**:4894–4903.
46. Li J, Yu M, Feng G, Hu H, Li X (2011) Breaches of the pial basement membrane are associated with defective dentate gyrus development in mouse models of congenital muscular dystrophies. *Neurosci Lett* **505**:19–24.
47. Li S, Jin Z, Koirala S, Bu L, Xu L, Hynes RO *et al* (2008) GPR56 regulates pial basement membrane integrity and cortical lamination. *J Neurosci* **28**:5817–5826.
48. Liu J, Ball SL, Yang Y, Mei P, Zhang L, Shi H *et al* (2006) A genetic model for muscle–eye–brain disease in mice lacking protein O-mannose 1,2-N-acetylglucosaminyltransferase (POMGnT1). *Mech Dev* **123**:228–240.
49. Longman C, Brockington M, Torelli S, Jimenez-Mallebrera C, Kennedy C, Khalil N *et al* (2003) Mutations in the human LARGE gene cause MDC1D, a novel form of congenital muscular dystrophy with severe mental retardation and abnormal glycosylation of alpha-dystroglycan. *Hum Mol Genet* **12**:2853–2861.
50. Manzini MC, Tambunan DE, Hill RS, Yu TW, Maynard TM, Heinzen EL *et al* (2012) Exome sequencing and functional validation in zebrafish identify GTDC2 mutations as a cause of Walker-Warburg syndrome. *Am J Hum Genet* **91**:541–547.
51. Marin-Padilla M (1971) Early prenatal ontogenesis of the cerebral cortex (neocortex) of the cat (*Felis domestica*). A Golgi study. I. The primordial neocortical organization. *Z Anat Entwicklungsgesch* **134**:117–145.
52. Marin-Padilla M (1998) Cajal-Retzius cells and the development of the neocortex. *Trends Neurosci* **21**:64–71.
53. Martinez-Cerdeno V, Noctor SC (2014) Cajal, Retzius, and Cajal-Retzius cells. *Front Neuroanat* **8**:48.
54. Meyer G, Cabrera Socorro A, Perez Garcia CG, Martinez Millan L, Walker N, Caput D (2004) Developmental roles of p73 in Cajal-Retzius cells and cortical patterning. *J Neurosci* **24**:9878–9887.
55. Michele DE, Barresi R, Kanagawa M, Saito F, Cohn RD, Satz JS *et al* (2002) Post-translational disruption of dystroglycan-ligand interactions in congenital muscular dystrophies. *Nature* **418**:417–422.
56. Moore CJ, Winder SJ (2010) Dystroglycan versatility in cell adhesion: a tale of multiple motifs. *Cell Commun Signal* **8**:3.
57. Moore SA, Saito F, Chen J, Michele DE, Henry MD, Messing A *et al* (2002) Deletion of brain dystroglycan recapitulates aspects of congenital muscular dystrophy. *Nature* **418**:422–425.
58. Muntoni F (2004) Journey into muscular dystrophies caused by abnormal glycosylation. *Acta Myol* **23**:79–84.
59. Myshrall TD, Moore SA, Ostendorf AP, Satz JS, Kowalczyk T, Nguyen H *et al* (2012) Dystroglycan on radial glia end feet is required for pial basement membrane integrity and columnar organization of the developing cerebral cortex. *J Neuropathol Exp Neurol* **71**:1047–1063.
60. Noctor SC, Flint AC, Weissman TA, Dammerman RS, Kriegstein AR (2001) Neurons derived from radial glial cells establish radial units in neocortex. *Nature* **409**:714–720.

61. Noctor SC, Palmer SL, Hasling T, Juliano SL (1999) Interference with the development of early generated neocortex results in disruption of radial glia and abnormal formation of neocortical layers. *Cereb Cortex* **9**:121–136.
62. Pilz DT, Matsumoto N, Minnerath S, Mills P, Gleeson JG, Allen KM *et al* (1998) LIS1 and XLIS (DCX) mutations cause most classical lissencephaly, but different patterns of malformation. *Hum Mol Genet* **7**:2029–2037.
63. Rakic P (1972) Mode of cell migration to the superficial layers of fetal monkey neocortex. *J Comp Neurol* **145**:61–83.
64. Roper SN, Abraham LA, Streit WJ (1997) Exposure to in utero irradiation produces disruption of radial glia in rats. *Dev Neurosci* **19**:521–528.
65. Roscioli T, Kamsteeg EJ, Buysse K, Maystadt I, van Reeuwijk J, van den Elzen C *et al* (2012) Mutations in ISPD cause Walker-Warburg syndrome and defective glycosylation of alpha-dystroglycan. *Nat Genet* **44**:581–585.
66. Saillour Y, Carion N, Quelin C, Leger PL, Boddaert N, Elie C *et al* (2009) LIS1-related isolated lissencephaly: spectrum of mutations and relationships with malformation severity. *Arch Neurol* **66**:1007–1015.
67. Sarnat HB, Flores-Sarnat L (2003) Etiological classification of CNS malformations: integration of molecular genetic and morphological criteria. *Epileptic Disord* **5** (Suppl. 2):S35–S43.
68. Sato S, Omori Y, Katoh K, Kondo M, Kanagawa M, Miyata K *et al* (2008) Pikachurin, a dystroglycan ligand, is essential for photoreceptor ribbon synapse formation. *Nat Neurosci* **11**: 923–931.
69. Satz JS, Ostendorf AP, Hou S, Turner A, Kusano H, Lee JC *et al* (2010) Distinct functions of glial and neuronal dystroglycan in the developing and adult mouse brain. *J Neurosci* **30**:14560–14572.
70. Shinozaki K, Miyagi T, Yoshida M, Miyata T, Ogawa M, Aizawa S, Suda Y (2002) Absence of Cajal-Retzius cells and subplate neurons associated with defects of tangential cell migration from ganglionic eminence in Emx1/2 double mutant cerebral cortex. *Development* **129**:3479–3492.
71. Solecki DJ (2012) Sticky situations: recent advances in control of cell adhesion during neuronal migration. *Curr Opin Neurobiol* **22**:791–798.
72. Stevens E, Carss KJ, Cirak S, Foley AR, Torelli S, Willer T *et al* (2013) Mutations in B3GALNT2 cause congenital muscular dystrophy and hypoglycosylation of alpha-dystroglycan. *Am J Hum Genet* **92**:354–365.
73. Sugita S, Saito F, Tang J, Satz J, Campbell K, Sudhof TC (2001) A stoichiometric complex of neurexins and dystroglycan in brain. *J Cell Biol* **154**:435–445.
74. Supèr H, Del Río JA, Martínez A, Pérez-Sust P, Soriano E (2000) Disruption of neuronal migration and radial glia in the developing cerebral cortex following ablation of the Cajal-Retzius cells. *Cereb Cortex* **10**:602–613.
75. Super H, Martinez A, Soriano E (1997) Degeneration of Cajal-Retzius cells in the developing cerebral cortex of the mouse after ablation of meningeal cells by 6-hydroxydopamine. *Brain Res Dev Brain Res* **98**:15–20.
76. Tamamaki N, Nakamura K, Okamoto K, Kaneko T (2001) Radial glia is a progenitor of neocortical neurons in the developing cerebral cortex. *Neurosci Res* **41**:51–60.
77. Toda T, Yoshioka M, Nakahori Y, Kanazawa I, Nakamura Y, Nakagome Y (1995) Genetic identity of Fukuyama-type congenital muscular dystrophy and Walker-Warburg syndrome. *Ann Neurol* **37**:99–101.
78. van Reeuwijk J, Grewal PK, Salih MA, Beltran-Valero de Bernabe D, McLaughlan JM, Michielse CB *et al* (2007) Intragenic deletion in the LARGE gene causes Walker-Warburg syndrome. *Hum Genet* **121**:685–690.
79. van Reeuwijk J, Janssen M, van den Elzen C, Beltran-Valero de Bernabe D, Sabatelli P, Merlini L *et al* (2005) POMT2 mutations cause alpha-dystroglycan hypoglycosylation and Walker-Warburg syndrome. *J Med Genet* **42**:907–912.
80. Vuillaumier-Barrot S, Bouchet-Seraphin C, Chelbi M, Devisme L, Quentin S, Gazal S *et al* (2012) Identification of mutations in TMEM5 and ISPD as a cause of severe cobblestone lissencephaly. *Am J Hum Genet* **91**:1135–1143.
81. Weiss KH, Johanssen C, Tielsch A, Herz J, Deller T, Frotscher M, Forster E (2003) Malformation of the radial glial scaffold in the dentate gyrus of reeler mice, scrambler mice, and ApoER2/VLDLR-deficient mice. *J Comp Neurol* **460**:56–65.
82. Willer T, Lee H, Lommel M, Yoshida-Moriguchi T, de Bernabe DB, Venzke D *et al* (2012) ISPD loss-of-function mutations disrupt dystroglycan O-mannosylation and cause Walker-Warburg syndrome. *Nat Genet* **44**:575–580.
83. Yang AC, Ng BG, Moore SA, Rush J, Waechter CJ, Raymond KM *et al* (2013) Congenital disorder of glycosylation due to DPM1 mutations presenting with dystroglycanopathy-type congenital muscular dystrophy. *Mol Genet Metab* **110**:345–351.
84. Yang Y, Zhang P, Xiong Y, Li X, Qi Y, Hu H (2007) Ectopia of meningeal fibroblasts and reactive gliosis in the cerebral cortex of the mouse model of muscle–eye–brain disease. *J Comp Neurol* **505**:459–477.
85. Yeo LY, Matar OK, Perez de Ortiz ES, Hewitt GF (2002) Simulation studies of phase inversion in agitated vessels using a Monte Carlo technique. *J Colloid Interface Sci* **248**:443–454.
86. Yoshida A, Kobayashi K, Manya H, Taniguchi K, Kano H, Mizuno M *et al* (2001) Muscular dystrophy and neuronal migration disorder caused by mutations in a glycosyltransferase, POMGnT1. *Dev Cell* **1**:717–724.
87. Yoshida-Moriguchi T, Willer T, Anderson ME, Venzke D, Whyte T, Muntoni F *et al* (2013) SGK196 is a glycosylation-specific O-mannose kinase required for dystroglycan function. *Science* **341**:896–899.